



Tanwear, A., Liang, X., Paz, E., Böhnert, T., Ghannam, R., Ferreira, R. and Heidari, H. (2022) Spintronic eyeblink gesture sensor with wearable interface system. IEEE Transactions on Biomedical Circuits and Systems, (doi: 10.1109/TBCAS.2022.3190689).

There may be differences between this version and the published version. You are advised to consult the publisher's version if you wish to cite from it.

<https://eprints.gla.ac.uk/273791/>

Deposited on: 29 June 2022

Enlighten – Research publications by members of the University of Glasgow
<http://eprints.gla.ac.uk>

Spintronic Eyeblink Gesture Sensor with Wearable Interface System

Asfand Tanwear, *Student Member, IEEE*, Xiangpeng Liang, Elvira Paz, Tim Böhnert, Rami Ghannam, Ricardo Ferreira and Hadi Heidari, *Senior Member, IEEE*

Abstract—This work presents an eyeblink system that detects magnets placed on the eyelid via integrated magnetic sensors and an analogue circuit on an eyewear frame (without a glass lens). The eyelid magnets were detected using tunnelling magnetoresistance (TMR) bridge sensors with a sensitivity of 14 mV/V/Oe and were positioned centre-right and centre-left of the eyewear frame. Each eye side has a single TMR sensor wired to a single circuit, where the signal was filtered (<0.5 Hz and >30 Hz) and amplified to detect the weak magnetic field produced by the 3-millimetre (mm) diameter and 0.5 mm thickness N42 Neodymium magnets attached to a medical tape strip, for the adult-age demographic. Each eyeblink was repeated by a trigger command (right eyeblink) followed by the appropriate command, right, left or both eyeblinks. The eyeblink gesture system has shown repeatability, resulting in blinking classification based on the analogue signal amplitude threshold. As a result, the signal can be scaled and classified as well as, integrated with a Bluetooth module in real-time. This will enable end-users to connect to various other Bluetooth enabled devices for wireless assistive technologies. The eyeblink system was tested by 14 participants via a stimuli-based game. Within an average time of 185-seconds, the system demonstrated a group mean accuracy of 72% for 40 commands. Moreover, the maximum information transfer rate (ITR) of the participants was 35.95 Bits per minute.

Index Terms—Spintronics, Tunnelling Magnetoresistance sensor, Eyeblink controller, user-machine interface, wireless assistive technology.

I. INTRODUCTION

Patient rehabilitation is an essential medical intervention designed to improve the quality of life of an individual experiencing limitations or impairments resulting from injury or congenital disabilities [1], [2]. In extreme situations, this may include limb replacement, with prosthetic arms or legs. Currently, these examples of prosthetics are being integrated with electronics to better interact or move within the modern world [3], [4]. Other methods that allow interfacing is through alternative muscle movements, where instead of limb replacement, eyeblink gestures can be used as a controller to

establish a human-device link. The ‘device’ may represent any digitally controlled system such as lights, wheelchairs, patient-carer communication interface or computers for human-computer interactions (HCI). By using eyeblinks as an input, individuals with non-functional limbs, e.g., Stroke victims or individuals with neural degenerative diseases, will be able to interact with electronic devices using both their right and left eyelids. The method is inclusive of the older demographic too, since human eye blinking deteriorates less with age [5], [6], but if the user-interface is sophisticated, e.g. language barriers or complex interface inputs, it may limit participation, thus keeping the user-interface simple will improve inclusivity.

Eyeblink gestures are also used for health monitoring, commonly used with Electrooculography (EOG) [7]. In the ophthalmology field, EOG detects eye movements and eyeblinks [8]. In fact, human blinking rate, duration and velocity at opened or closed eyelid positions have been used to determine human physiological traits that include sleep cycle, focused attention and fatigue/tiredness. [9], [10]. Due to its reliability issues and the need for probes to be attached to the participant’s face, setup time with EOG is typically high. Therefore volunteer participation may be limited, which will affect the quality and statistical accuracy of a study that best represents a general population [9]. Additionally, EOG detects artefacts from skeletal muscle movements and requires post signal analysis for data classification [8]. Typically, accurately determining signals from a raw dataset requires experienced clinicians for post-processing, which can delay results, mainly when multiple tests are conducted on multiple participants [11], [12]. Therefore, an alternative method is required that offers better mobility and reduced setup time, for more inclusion of the target medical demographic.

A contact-free alternative for eyeblink detection can be based on near-infrared emitters and cameras. Due to their high energy demand, high cost (\$10,000 approx.) and large size, desktop-based infrared eyeblink detectors e.g. Eyelink 1000, are primarily used in clinical trials and found with limited use in other applications [13], [14]. State-of-the-art mobile eye-tracking cameras such as the Tobii Glasses, which can also monitor eyeblinks, require a wired connection to a battery unit due to their high energy consumption [15], [16]. These camera-based approaches are sensitive to ambient light, hindering their application in wearable devices. Whilst the embedded miniaturised high-resolution camera makes them expensive, sometimes twice as much as the desktop versions [17]–[19]. The prohibitive cost of such systems makes it difficult for more comprehensive public access, and once again, this option will limit the diversity of users.

This work was supported by MAGMA project (n. 1849) from Royal Society of Edinburgh, Leverhulme Trust (SAS-2020-045), and the UK EPSRC DTP under grant reference 2126385. (Corresponding authors: Hadi Heidari.)

A. Tanwear, X. Liang, R. Ghannam and H. Heidari are with James Watt School of Engineering, University of Glasgow, G128QQ Glasgow, United Kingdom. (e-mail: a.tanwear.1@research.gla.ac.uk Hadi.Heidari@glasgow.ac.uk)

T. Böhnert, E. Paz, P. P. Freitas, R. Ferreira are with International Iberian Nanotechnology Laboratory (INL), 4715-330 Braga, Portugal (email: Ricardo.ferreira@inl.int).

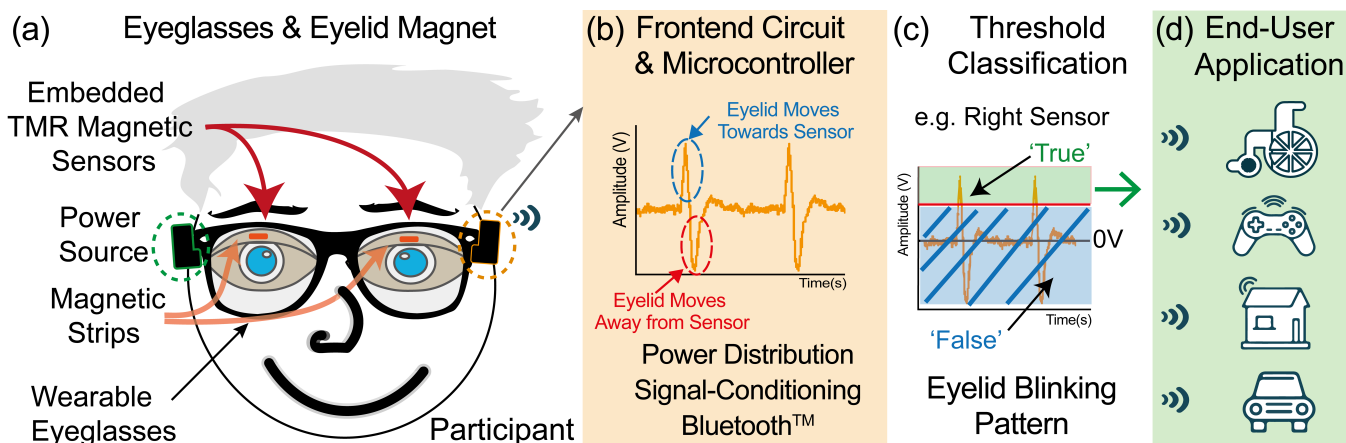


Fig.1. (a) Shows an illustrated participant wearing magnetic strips that are attached to the eyelid and are detected by Tunneling Magnetoresistance (TMR) embedded sensors. (b) Illustrates an example of a signal when eye blinking, it is the output of the eyewear circuit including the Bluetooth low energy (BLE) device. The gestures are detected when the participant blinks either left, right, or both eyelids towards the sensors, positioned on the right and left of the eyewear frame. (c) Demonstrates how the gestures are classified on the computer when amplitude thresholds are met. (d) Shows examples of end-user applications of an eyeblink gesture controller, which allows the participant to wirelessly control electronic systems, this includes gaming, wheelchair, car, and home interface.

This paper demonstrates a low power, wearable, lightweight, high accuracy eyeblink gesture detector, with magnets sized to fit the eyelids of the adult-age demographic. As illustrated in Fig.1, the system is accessible to a broader population by maintaining low-cost and allowing flexibility for different interfacing options. The method first proposed in Tanwear *et al.* [20], showed the magnetic field and circuit simulation results for eyeblink gesture detection using magnets as the source, and Tunnel magnetoresistance (TMR) sensors for detection. The simulation results analysed the magnetic field at different separations. The signal response at 2-2.5 centimetres demonstrated large signal amplitudes at the output, when simulating a blink, and showed that it can be classified, using threshold classification.

In this paper, the wearable eyeblink detection system is presented, as well as the methodology for creating the device. Information about the experimental setup and results are also presented and analysed. The limitations of the proof-of-concept will be discussed as well as future work to address the limitations. The paper then reintroduces the novelty and summarizes the main takeaways within the conclusion.

II. METHODOLOGY

A. Magnetic Strip Fabrication (Source)

A strong neodymium permanent magnet (F300-50, First4Magnets UK) was attached to medical tape and then stuck on the eyelid. The aim was to have a sufficiently high magnetic field strength, capable of being detected by a sensor maximally 2.5 cm away [20]. The magnetic field at the surface of the magnet was rated by the manufacturer as 1500 gauss or 150 milli-Tesla (mT), whilst any separation would reduce the field considerably due to the inverse square law [20]. Hence, the magnetic field at the maximum sensor separation was approximately 1 micro-Tesla (uT).

The magnet was 3 mm in diameter and 0.5 mm in thickness. The magnet size was based on the typical size of the eyelid crease height (Vertical dimension of the palpebral fissure) being less than <6.5 mm average [21], and when closed it was at 2 mm average. The eyelid width (horizontal dimension of the

palpebral fissure) varied slightly more depending on the demographic (race and age); for example, between African (up to 10 mm) and Caucasian descent (up to 12.8 mm), the measurements are based on the doubling of the apex distance from Price *et al.* [22]. The area where it was suitable to have an object on the eyelid was smaller than the effective area of the eyelid. Therefore, the aim was to have a magnetic source as small as possible. Research studies such as Park *et al.* [23] on participants from east-Asian descents do not explore comparisons between different ethnicities, so to ensure inclusivity, further studies are required to investigate the effective area where a magnet can safely and comfortably be placed on an eyelid for different eyelid shapes and sizes. Meanwhile, this study had kept the magnet around 3 mm and 0.5 mm diameter, to be compatible with adult eyelids from the demographics mentioned earlier. The magnet weighed 30 milligrams (0.03g) as not to impede any natural eyeblinks and be discomforting for the user. The thin 0.5 mm profile of the magnet, allowed the eyelid to fold when the eyes were open, as the medical tape with the magnet would increase the thickness to ~0.7 mm. The medical tape (Papal Microporoso by EROSKI) was cut to a size of ~5 mm in width and 10 mm in length. From initial feedback with the magnet and tape, the participant did not feel the presence of the magnetic strip, however, this was dependent on the location on the eyelid. In this study, the lower part of the eyelid, whilst not touching the eyelash itself, was found to be the best location of the magnet. When placed at the upper eyelid and when the eye is open, the magnetic strip would pull on the eyelid as the eyelid was folding, which may cause the participant to feel the medical tape.

The sensor would also detect other field sources, such as the static earth's magnetic field and manmade environment field. The earth's magnetic field was found to be between 35 to 60 micro-Tesla. The manmade magnetic field, typically found at high radio frequencies, or power lines (50-60 Hz) generates magnetic fields at the nano-Tesla range or smaller [24]. If the sensor moved >1 centimetres (cm) in any direction, the sensor was not able to distinguish an eyeblink from the external environment fields due to similar field strengths. It must be

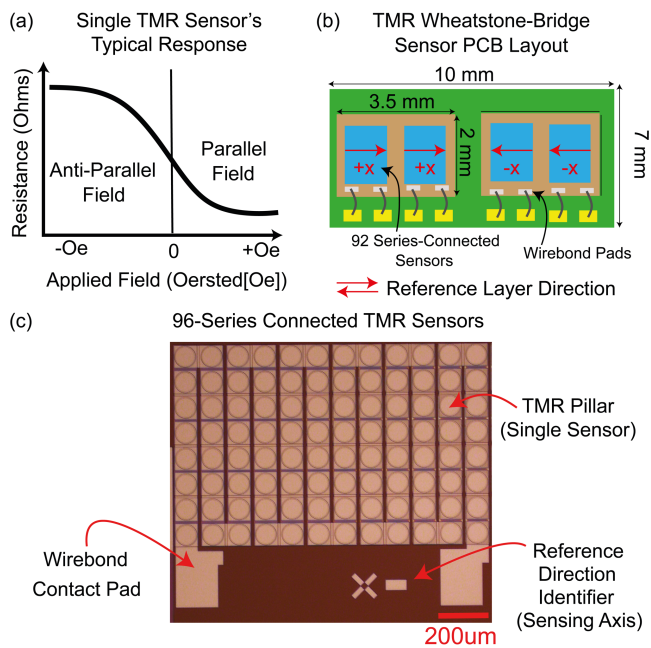


Fig.2. (a). A typical TMR magnetic sensor response is shown, where anti-parallel external field with respect to the reference layer will increase the resistance until saturation. Whilst parallel external fields will decrease the resistance, also until saturation. The gradient of the response will determine the sensors sensitivity when biased (current or voltage). (b). The figure shows a PCB used for each-eye side. Where each PCB contains two chips and within each chip contains 2 x 96 series connected TMR sensors with the same reference layer direction. The two chips are anti-parallel to each other. Each chip is 2 x 3.5mm where the PCB containing the wire-bond pads is 7 x 10 mm. (c). Shows a closeup of the 96-series-connected sensors, with reference direction towards the left (minus X-axis).

noted that if the eyewear frame moved slowly then little or no fields were detected due to the high pass filters in our system. To circumvent detecting natural eyewear movement, a trigger command was used, since if the eyewear moved, both sensors would detect it at the same time. Having a single eye-trigger (wink) command will ensure that the system would detect eye commands. However, this does mean that the user must keep minimal head movements after the trigger command.

Magnetic field produces non-ionizing radiation that can be found everywhere and its impact on public health is still not clear as, for example, miscarriage [25], but there are safety limits that must be adhered to. The magnetic field strength of the source limits the choice of the magnet. The International Commission on Non-Ionizing Radiation Protection (ICNIRP) recommends that the body exposure limit for the public should not exceed 400 milli-Tesla (mT), whilst an individual with a pacemaker at a maximum of 0.5 mT [26]. As a precaution, no individual with a pacemaker was invited to participate in the test until in-depth clinical studies are conducted. To reiterate, the magnet (150 mT) was below the exposure limit of ICNIRP for the public without pacemaker.

According to the World Health Organisation (biological effects), general eye irritation may occur if the source is a microwave or a high frequency electromagnetic wave [27], therefore, a magnet was used to generate this field. As it is a static source, that when moved with respect to the sensor will equate to a low frequency signal ~a few Hertz. The static field can also be produced by a coil. However, a large power source would be needed, to create a detectable field or it will need more

coil turns to reduce the power consumption, both options will be difficult to fit on an eyelid.

B. Sensor Fabrication

The spintronic TMR sensor, also referred to as magnetic tunnel junctions, had its stack deposited in a Singulus Timaris physical vapor deposition (PVD) system, with a base pressure of 2×10^{-8} mbar. To obtain a linear response for the TMR pillars, the stack had a weakly pinned free layer [28]: Buffer / 20 IrMn / 2 CoFe₃₀ / 0.7 Ru / 2.6 CoFe₄₀B₂₀ / MgO [15 kΩ μm²] / 2 CoFe₄₀B₂₀ / 0.21 Ta / 6 NiFe / 0.2 Ru / 6 IrMn / capping (all the thickness in nm). The sensor's signal to noise ratio (SNR) is proportional to the square root of the TMR area and the number of TMR pillars in series [29], [30]. To maximize the SNR, a series of 96 pillars with a diameter of 100 micrometres (μm) was fabricated, the biggest possible due to the space limitation of the eyewear [31]. These sensors are good candidates for eyeblink detection because of their high sensitivity and low power consumption [29], [31], [32].

For the eyeblink application, the sensor was designed to detect small fields with a maximum magnitude of 10 Oe, with good linearity and almost negligible coercivity. The sensor was linearized in the region between ± 50 Oe through a two-step annealing process [28]. In the first step, a strong 1 T field was applied parallel to the reference direction with 330 deg. C, for 2 hours. The second annealing step was 270 deg. C, and a 0.5 T field was applied orthogonal to the reference direction for 1 hour.

Four of the 96 series-connected TMR, with a total resistance of 207 ohms each, were connected in a Wheatstone bridge configuration on a printed circuit board (PCB) through aluminium wedge wire-bonds. As illustrated in Fig. 2, two chips with anti-parallel reference directions to each other, contain two of the 96 series connected TMR and are mounted in a bridge configuration. The Wheatstone bridge minimised temperature drift, only if one whole or both whole chips were affected, it meant that any temperature change would not vary the bridge's output signal [33]–[35]. The sensors were placed at least 2 cm away from an individual, away from the majority of the body heat source. When the device temperature is changed it would still affect the noise levels such as thermal noise [31]. The total noise including thermal noise, was measured to be around a few milli-volts whilst the blink signal would be between 1 to 3.3V. Any ambient temperature variation will change the Johnson noise levels around the nano-volts, possibly up to microvolts range, and with amplification of 100, up to a few millivolts of change is possible with extreme heat variations. However, the SNR of the system will remain large, if the magnetic source continues to generate strong magnetic fields.

The TMR bridge sensor is connected to the eyeblink circuit, as illustrated in Fig. 3. The sensor's sensitivity was 14 mV/V/Oe and had a measured working field range of at least ± 12 Oe (1.2 milli-Tesla) with coercivity around 0.1 Oe, as shown in Fig. 4. The sensor PCB size was 7 x 10 mm whilst each chip was 2 x 3.5 mm. One bridge sensor was positioned on the right-hand side of the eyewear's lens frame, whilst the other on the left, as shown in Fig. 5. When an eyewear was worn by the participant, the sensors were up to eyebrows height, otherwise any lower would block a participant's view.

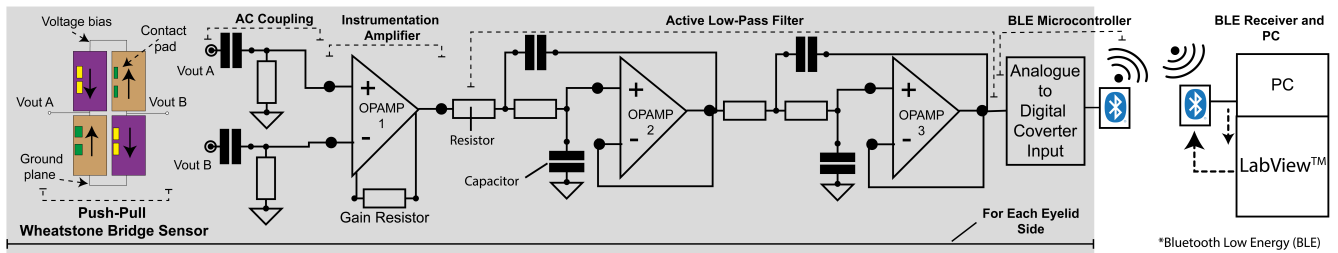


Fig.3. The circuit diagram illustrates that the push-pull bridge magnetic sensors have two outputs, both are AC Coupled to remove DC offsets and is cut-off at 0.53Hz. Amplification was provided by the instrumentation amplifier, followed by an active low-pass filter to attenuate frequencies above 30 Hz. The signal was received by the Bluetooth low energy (BLE) microcontroller via the Analogue to Digital Converter (ADC). Both eyelink sensors have individual ADC inputs that was then transmitted via Bluetooth to the computer (PC) and the interface programming software LabVIEW.

C. Eyewear Design

A participant wearing the eyewear is shown in Fig.5(a), as well as the location of the sensors in Fig.5(b). Where in Fig. 5(c) shows the magnetic strips on the eyelid. They were approximately 2.5 centimetres away from the sensors, which were on the wearable eyewear. The TMR sensors are positioned at the top-centre corner of each side of the eyewear frame and are wired to the front-end circuit. The eyewear was a custom-built 3D Thermoplastic polyurethane (TPU) eyewear, which have the dimensions of an adult's optical glasses and were designed to allow the magnetic sensors to be placed facing the eyelid, without obstructing the person's vision.

The design of the eyewear is shared in the appendix. Using TPU flexible filament, the eyewear was fabricated within 9 hours where the total area of the eyewear was $145.5 \times 160.1 \times 56.2 \text{ mm}^3$. The filament density of the eyewear was 40% and used 77 g of the filament, as this included supports and raft. The eyewear weighed 50 g, while the fitted eyewear was 100 g. A few extra grams may be added in the future to protect the eyewear e.g., waterproofing and for appearance enhancement. The eyewear's lens area was 8 mm thick, which makes the frame more bulky than regular glasses, as the aim was to maintain a strong structure. Different users with different head size shapes would use the same eyewear within this study and

the prototype had to withstand the stress and strain of continual usage.

The aviator shape lens frame was 33 mm in height and 55 mm in width. The length of the glasses was 160 mm, this includes the over-ear frame. The over-ear of the eyewear (45 mm in length) was shorter and thicker than conventional eyewear as it was difficult to decrease the thickness (6 mm) of the eyewear at the ear side. If the eyewear were made from 'Hard Plastic', more slim profiles would be possible using conventional non-3D printed manufacturing methods.

The allocated PCB area was 86.92 mm in length and 34 mm in height. The PCB area tapered down to 21 mm when approaching the ear-side, as shown from Fig.5(a). Since the electronics that were attached onto the eyewear side did not heat up, no extra filament was necessary for thermal padding. The components that were most at risk to run hot e.g. (voltage regulators) were facing away from the user/eyewear and towards the air.

D. Eyeblink Speeds and Signal Bandwidth

The aim of the eyeblink system was to detect voluntary blinking from both eyelids as interface commands [36]. In other words, the right, left or both eyeblinks. Initializing the system required an eye-trigger command, this was set as the right eye. As mentioned previously (magnetic strip fabrication), the trigger allows the user to move without generating commands unintentionally. Another benefit of the single eye-trigger is that any unconscious blinking with both eyes and winking of the non-trigger eye, prior to the trigger is ignored. After triggering however, it does briefly require some mental focus to prevent the next single blink or wink command to be an unintentional command. Therefore, the trigger aims to make the system user-friendly by allowing a user to naturally blink and move without generating unwanted commands.

Any eyeblink would generate a bipolar signal (AC), depending on whether the magnetic field is parallel or anti-parallel to the sensor's reference layer. The amplitude depended on the detected field strength, sensor sensitivity and speed of the eyeblinks. Since the analogue system has filters, it is important to generate eye blinking frequencies within the pass band (0.53-30 Hz).

From the literature, the frequency of involuntary blinking was approximated with an estimated average and the standard deviation of the blink rate (BR) was 18.27 ± 10.44 blinks per minute [37]. From a second source tested with patients with or suspected with glaucoma, the BR is defined as eyelid closures duration between 50-500 ms and showed a blink rate between

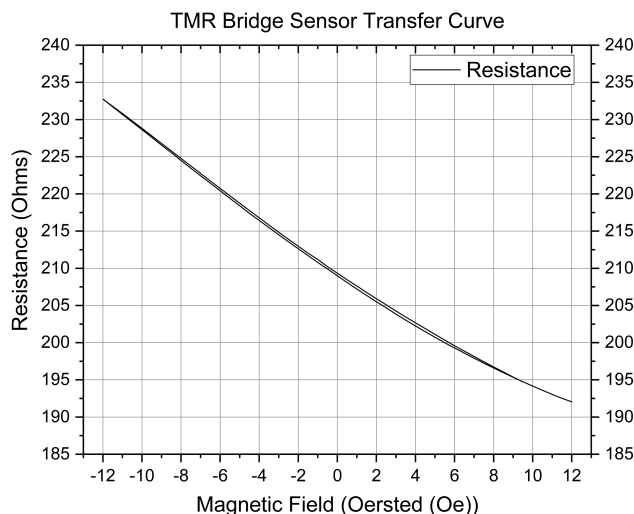


Fig.4. The image shows the measured resistance response to the external magnetic field of the TMR bridge sensor, when tested between +/- 12 Oe (1.2 milli-Tesla) with around 0.1 Oe coercivity. The same sensor was used for the eyeblink gesture application in this study.

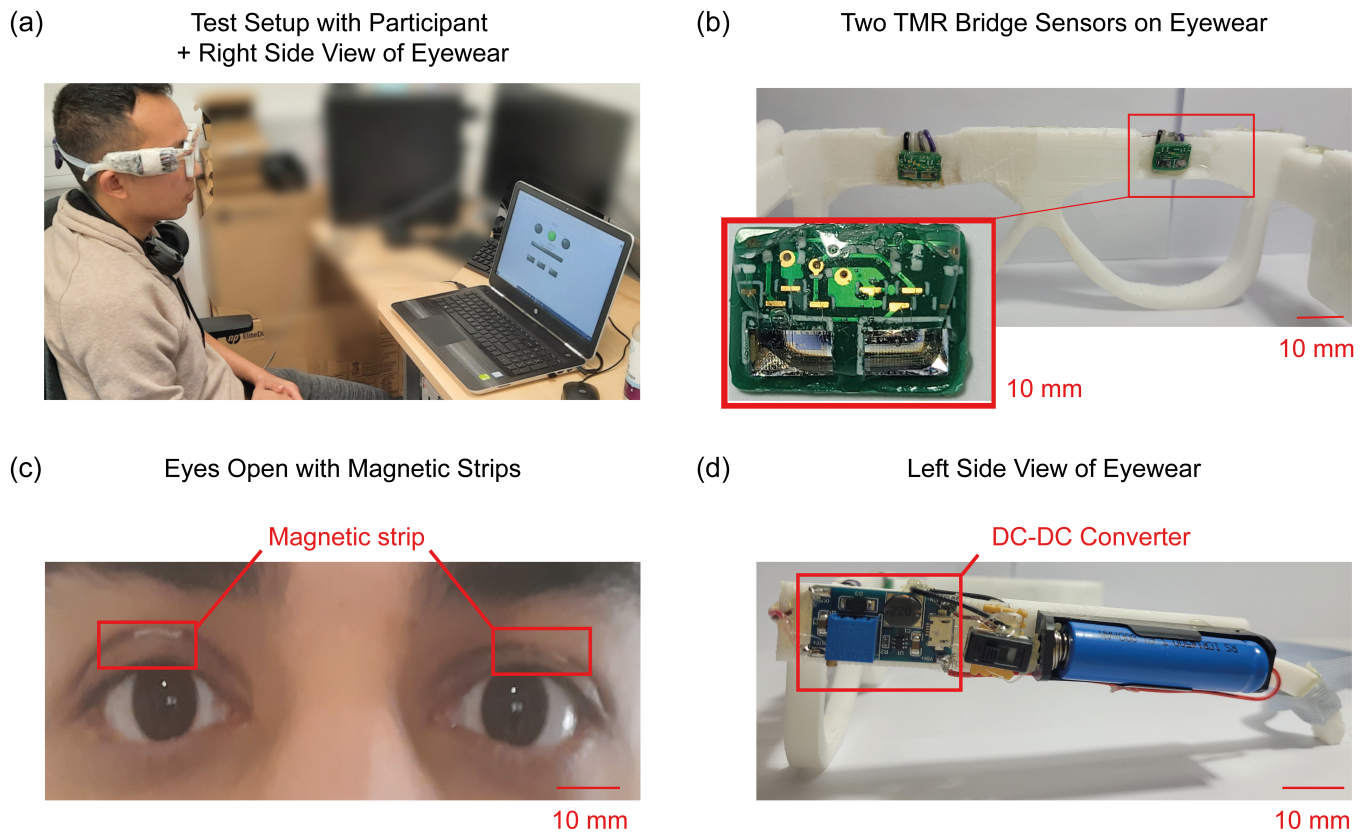


Fig.5. (a). Shows an image of a participant undertaking the stimuli-based game, using the eyblink gesture system. The image also shows a right-side view of the eyewear showing the PCB covered with a plastic protective film. (b). Shows the back view of the eyewear, revealing the position of the Wheatstone bridge. (10×7 mm). The inset image is the closeup of a bridge sensor PCB (c). Shows an individual wearing an eyelid magnetic strip (10×5 mm) with the eyes open (d). Is an image of the left side view of the eyewear showing the battery, switch, and DC-DC converter circuit board (without protective plastic film).

9 and 13 blinks per minute [38]. Blink rate does not represent the speed that the eyelid would travel during either voluntary or involuntary blinks (including reflex blinks) i.e., the frequency of the eyblink magnetic field signal detected by the magnetic sensor. For example, having a blink rate of 18 means that there will be 0.3 blinks per second, so the frequency would then be 3.33 Hz, the eye is not continually moving, in other words not then completing 0.3 of an eyblink per unit second of time. Assuming eyblink has constant speed due to their unconscious periodic behaviour [39], then the duration of an eyblink may correlate to the frequency of the signal detected by the sensors. Hence, if the involuntary eyblink duration is 500 ms it would translate to 2 Hz and up to 20 Hz for 50 ms. This is based on the time-period and frequency formulae, where time-period (seconds) = $1/\text{frequency}$ (Hertz, Hz).

In the extensive 2013 study by Kwon *et al.* [39] only the voluntary eyblinks were examined from healthy individuals, the speed of an eyblink when closing is faster than opening by approximately two times the speed. This suggests, at least when considering voluntary eyblinks, speed is not constant. The duration of a voluntary eye closure is reported to be 58 ± 4 ms, hence based on the duration, the frequency is ~ 17 Hz, whilst the opening of the eye lasts 273 ± 23 ms or 3.66 Hz. Also, in one instance in the study to fully open the eye, the individual took 572 ± 25 ms, where the individual took 299 ms to open 97 % of the eye. If 572 ms is considered, then the minimum frequency

of eyelid movement is 1.74 Hz otherwise, it will be around 3.66 Hz.

Therefore, based on the literature, voluntary eyblink (1.74 Hz to 17 Hz) and involuntary eyblink (2 Hz to 20 Hz) cannot be separated in the frequency domain due to overlap. This information was used to improve the SNR, as the sensor detects magnetic fields across a large frequency bandwidth and will pick up low and high frequency fields. The rejection of high frequency noise > 20 Hz ensures that the signal was much smoother by removing fast magnetic fields, whilst having a high pass filter < 1.74 Hz ensured to remove any DC drift e.g., thermal drift and any minor movements e.g., eye twitch.

E. Front-End Circuit Design

The magnetic field requires an analogue circuit capable of amplification, driving the analogue to digital converter (ADC), and noise reduction. Noise for this application can originate from the electronics and external magnetic field noise. The design aimed to achieve a high SNR and classify eyblink with threshold-based classification. The following section explains the circuit shown in Fig.3. in detail:

Input: The Wheatstone bridge TMR sensor has two terminals for differential output and requires a difference operational amplifier with a high input impedance and as such, an instrumentation amplifier (INA818AID, Texas instrument) was used. If a regular difference amplifier was used, the impedance variation prior to the operational amplifier, will lead to

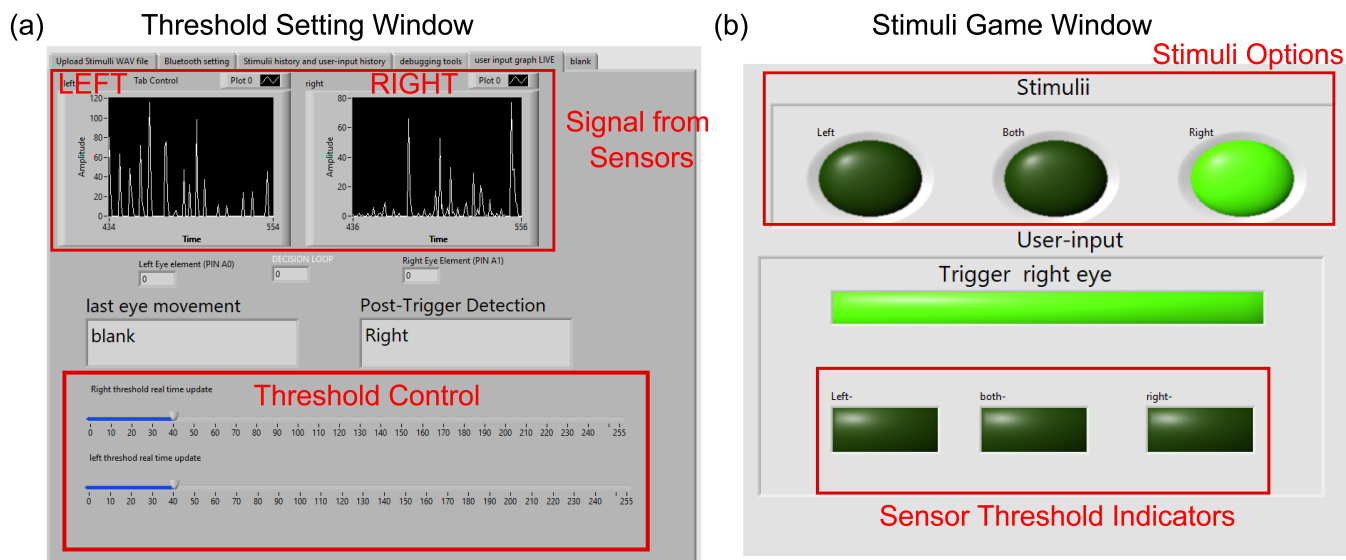


Fig.6. (a) Shows the time domain response of the left and right sensors, as well as the mechanism to set the threshold. This LabVIEW window was not shown to the participant during the trials. (b) Shows the LabVIEW window that was shown to the participants during the trials, where the stimuli LEDs were at the top of the window. The trigger LED was in the middle and the sensor threshold indicators were at the bottom of the window.

instability and produce non-reproducible signals. The instrumentation amplifier subtracted the difference between output A and B and amplified the signal. Using a single 500-ohm resistor the gain value was set to 100, this along with a high CMRR (Common Mode Rejection Ratio) will ensure noise from the circuit is comparably smaller, hence ensuring sufficient SNR for reproducible classification.

High Pass Filter: Before the input of the instrument amplifier, a passive high passive filter was present at both inputs A and B. A 1 micro-Farad capacitor in series with the respective signal path blocked DC signals and allowed the AC signal to pass through. A 300 kilo-Ohm resistor was needed to allow current flow to the input of the operational amplifier. The resulting -3 dB point i.e., the 50% power loss cut-off frequency was set to 0.53 Hz. Frequencies slightly above will be attenuated and the signal at 0.53 Hz will have 29% voltage attenuation and 1% attenuation at 1 Hz. Hence for voluntary eyeblink bandwidth (1.74 - 17 Hz) this is then sufficient.

Low pass filter: After the amplification stage, a Sallen-key active low-pass filter was used to provide a Butterworth frequency response. This provided -3 dB attenuation at 30 Hz and -18 dB at 50 Hz. This was to ensure that the manmade 50 Hz magnetic field was heavily attenuated, whilst 17 Hz signal frequencies is not, e.g., 20 Hz had an attenuation of -0.18 dB. The operational amplifier (OPA2188 by Texas instrument) was used to implement active filtering as it provided low DC offset (maximum 25uV), and low noise 8.8nV/ $\sqrt{\text{Hz}}$ at 1 Hz. Due to low DC offset, no additional step was required to remove it, e.g., high pass filter.

BLE-Microcontroller: A 2.4 GHz Bluetooth low energy (BLE) microcontroller device (Adafruit Itsy-bitsy nrf52840) was used for interfacing with a computer, with current consumption up to 11 mA when biased at 5V. The ultra-light device is weighed at 3 grams and was sized, 36.0 mm x 17.6 mm x 5.3 mm. The board had detected and read analogue signals from 0 V to 3.3 V. The bipolar signal below zero volts was not read. However, the classifier still detected eyeblinks

even though the micro-controller could not record the entire motion. To read signal amplitude up to 3.3 V, this required that the power input should be at least 3.5 V up to 6 V, a 5 V bias was then chosen to ensure power stability.

Power unit: As shown in Fig.5(d), the entire system was powered by a single 3.7 Volts nominal 0.8 Ampere-Hour battery, providing battery life of at least 6.6 hours of continuous usage. The power consumption was 0.455 Watts (W) at 3.7 V with a current at 0.125 Ampere (A), with peak consumption during a blink was at 0.18 A (0.67 W). An AA-size battery holder was used and plugged into a 12V step-up voltage converter (MT3608-2A). The 12 V was converted to split supply ± 6 V using a voltage divider; this however does increase current consumption but allows flexibility by altering the resistance. Using the step-up converter resulted in a high-frequency signal noise, around 20 milli Vpk-Vpk, with random spikes up to 200 milli-Volts (mV). This was mitigated by using 2 x 3.3V regulators (LP2992AIM5-3.3), a negative 3.3 V (TPS72301DBVR) and a 5 V regulator (LP2992AIM5-5). The noise was then reduced to 8 milli Vpk-Vpk with high frequency noise spikes removed.

F. Calibration and Classification

Typically, magnetic sensors are calibrated by balancing resistors to remove any DC offsets or are calibrated to zero fields digitally, at the readout system. In this system, any DC offset e.g., from earths static magnetic field or from the bridge sensor itself (imbalanced bridge sensor) was filtered using a high pass filter, as only eyeblink movements needed to be detected. Moreover, since the magnitude of the magnetic field information was not required to detect the changing fields, the sensors were not calibrated to zero fields digitally.

The eyeblink signals were classified using amplitude threshold classification received at the computer via Bluetooth, as illustrated in Fig.1. Any movement generated peak/triangular signal (as shown in Fig.6(a)), and based on the amplitude threshold, it can be considered an eyeblink, where each of the two bridge sensors may generate slightly different output from

an eyeblink, and thus the threshold is set manually for classification. Each participant with respect to the sensors will have slightly different location of the magnets resulting in varying signal amplitudes; therefore, threshold calibration is an important step before testing. It must be noted that the magnetic field from the neighbouring eyeblink was also detected by the sensor. This was due to high sensitivity and strong source fields; the threshold was increased to classify the localized eyeblink only. The default threshold value was 60% of the peak signal when blinking. If the incoming amplitude was too small, the user was asked to adjust the magnet and align it with the sensors for maximum field detection. Again, care is needed to ensure that a neighbouring eyeblink does not trigger the sensor. Otherwise, the threshold is manually increased. Also, the threshold is not set near zero to avoid triggering the sensor from electric noise, magnetic field noise or a signal from a neighbouring eyeblink.

The 3.3V signal was digitised and transmitted via Bluetooth to a laptop PC (HP RTL8723BE, Intel i5 2.5GHz, 4GB RAM), the signal was translated to an 8-bit integer from 0-255 points at a baud rate of 115200. The signal was processed, classified, and the interface was developed using LabVIEW 2020. Fig.6(a) shows the digitised signal from the sensors in LabVIEW, where the signal was graphed at around a 100-millisecond delay and the threshold value was set manually.

The threshold-based classification algorithm had read signals from the left and right eyes separately but simultaneously. This meant that incoming signals from the right and left eyes can have different threshold values and are set manually. Moreover, both can be triggered together when both eyes blink. A 375-millisecond time window was set in LabVIEW to classify each or both eyeblinks. This was important, since one eye would reach the threshold value quicker when blinking both eyes.

When a person blinked, a bipolar peak was observed at the final stage of the analogue front-end. Depending on the detected magnetic field, the amplitude can reach up to rail-to-rail supply voltage of the operational amplifiers ± 3.3 V. The Bluetooth module is a single supply device, where the AC signal below zero volts was cut-off. Therefore, as previously mentioned this means the module does not record that full motion. Depending on the source field polarity with respect to the sensors reference direction, either opening or shutting of the eye was detected, in some cases both can be detected. This was because the sensor and magnet were not perfectly aligned. In either case, missing motion data will not impact the system, as the aim of the system was to detect blinking, irrespective if the eyelid was shutting or opening the eye when the signal was detected.

G. User Interface Communication

Communication between LabVIEW 2020 user interface and the eyeblink circuit was achieved by a USB Bluetooth module (BLED112-V1 from silicon labs). This enabled the PC to connect to the Bluetooth low energy eyewear device. In fact, LabVIEW BLE toolkit, mentioned in the Appendix, allowed the LabVIEW software to communicate wirelessly with our device. Typical Bluetooth technology in PCs is incompatible with our system. However, mobile phones allow communication with our BLE eyeblink devices. Alternatively, Wi-Fi based communication modules offer faster data

transmission. However, establishing multiple Wi-Fi connections on a single PC is not always possible since the connection is usually used for internet connectivity. Otherwise, a separate Wi-Fi adapter is needed. Also, a Wi-Fi-based controller typically consumes more power to accommodate faster information processing and transfer at longer ranges. Whereas a BLE device has little power consumption (50 milli-Watts), and an internet Wi-Fi connection can function concurrently.

III. EXPERIMENT SETUP

In the following section we describe our experimental setup, which has been adapted from Graybill *et al.* [36]. During our experiments, each participant was invited to sit down and play a stimuli-game to determine system performance metrics.

A. Participant Group Selection and Test Environment.

The system was assessed by 14 participants who volunteered to take part in our experiments, participants were both males and females aged between 21 and 35. An adult age demographic was chosen, since the 3 mm diameter magnets could be large for children. Children may also find the trials developed for this test fatiguing and may lose interest in the game before completion. None of the participants (except those wearing pacemakers) were rejected during the process or selected with 'ability' for this study. The ability referring to being able to individually wink with either eye.

B. Interface Test Setup and Training

To assess the performance of the eyeblink system, a stimuli-based game was created, where the participant would practice the game until completion before being recorded for the three trials. The participant would sit down in front of a laptop with LabVIEW open and will turn 'ON' the eyewear. The game will start when the LabVIEW application is running, and after a delay of around 10 seconds the program should have established a Bluetooth connection to the microcontroller. The stimuli program will select one of the three eyeblink options, and when it was selected, a circle will be lit up, referred to as LED in LabVIEW. An audible robotic voice played the words 'Left,' 'Right' or 'Both' at each iteration. A separate row had four LEDs, with an extra LED for the 'Trigger' command, activated by the right eye (default). This allowed the participant to visually check if the trigger had been activated and that the next eyeblink was a stimuli command.

The purpose of the trigger was to allow natural head movements and unintentional eyeblinks, as a single eye was used as a trigger (right eye), as explained earlier. Once the participant blinked after the trigger, it did not matter if it was correct, incorrect, or if they moved their head, since the data was still being recorded before the next stimuli was presented. The system waits until no eyeblinks are detected, after the time of triggering and the next detected eyeblink is the recorded command. This prevents the game to accidentally register the trigger command as being a stimuli command.

The game randomly selected three eye-blink stimuli options (Right, Left and Both), up to 20 times. The number of commands of the same eyeblink will be random to makeup the

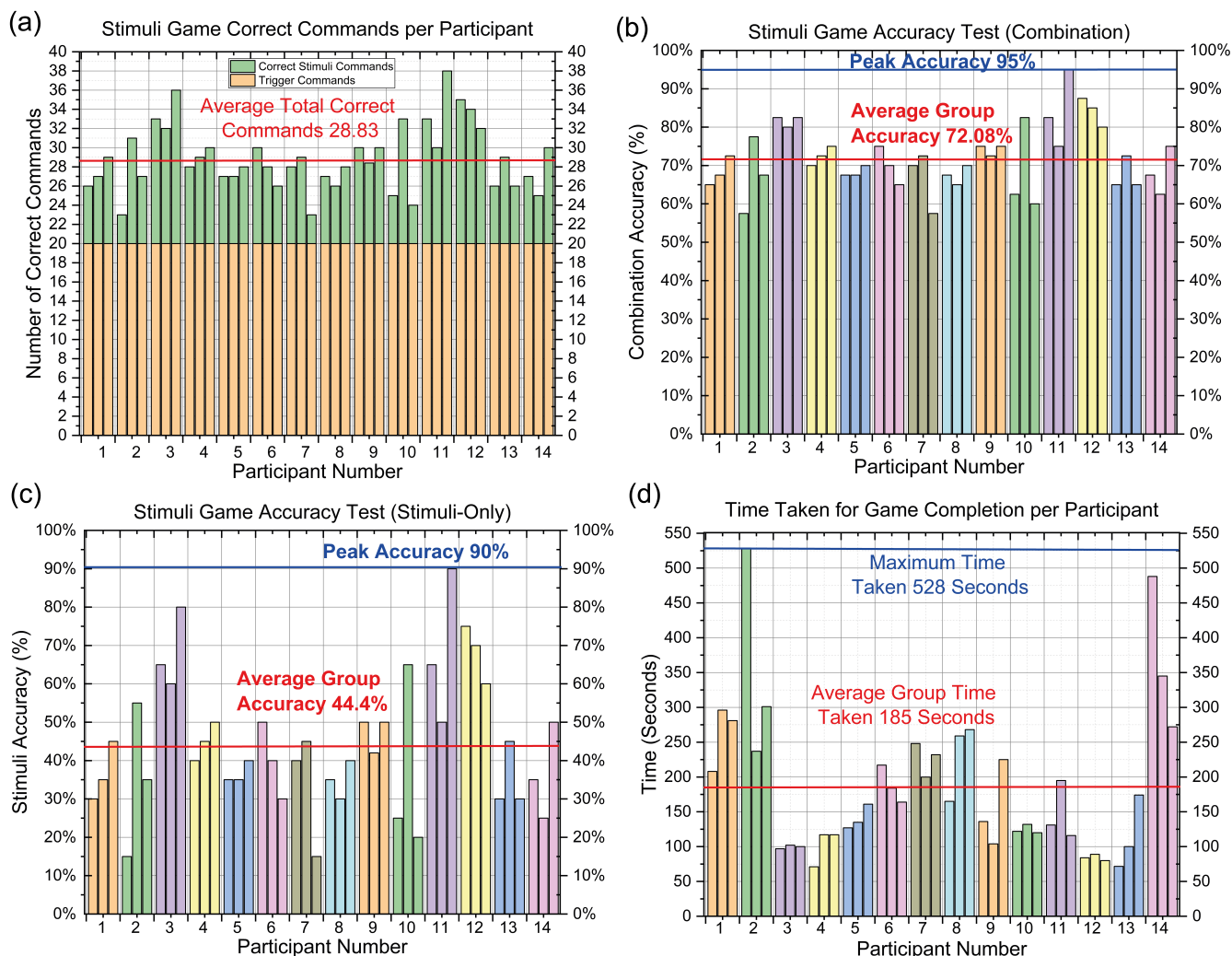


Fig.7. (a) Shows the number of trigger and correct stimuli commands, per participant and in the order of each trial (out of 40 commands). The mean number of correct commands was 28.83 for the group. (b) Shows the combination accuracy (%) of the stimuli game, where both trigger and stimuli commands were considered per participant. The mean accuracy of total commands of the group was 72.08 %. (c) Shows the stimuli-only accuracy (%) of the stimuli game, where only the stimuli commands were considered per participant. The mean accuracy of stimuli-only commands was 44.4 % for the group. (d) Graphs the time taken in seconds for each participant to complete each stimuli game trial (40 commands). The groups mean time taken to complete each trial was 185 seconds.

20 stimuli commands. This was to ensure that the game was random, even if the participant had replayed the game, for example during training of the system. The total number of commands was 40, as this included the 20 trigger commands and the 20 stimuli commands. Before the trial was recorded for the study, the first process was to adjust the amplitude threshold whilst the participants were practising the game. The threshold adjustments were made by the researchers from this study, where the aim was to ensure that any eyeblink would trigger the correct sensor and not the neighbouring sensor unintentionally. The participant had to at least complete one practice trial session (40 commands) before attempting three trials that were recorded for this study.

The system had two sets of accuracy standards called ‘combination’ accuracy and ‘stimuli-only’ accuracy. Where the combination accuracy was a measure of both the trigger and stimuli commands i.e., 40 commands. For example, zero accuracy would be achieved in the case that the participant could not ‘Trigger’ using their right eye and was not able to finish the 10-minute game. If the participant did manage to

finish the game within the limit, then the minimum combination accuracy was 50%. In contrast, the stimuli accuracy was a measure of how accurately the participant matched their eyeblink to the given stimuli i.e., 20 commands. The two different accuracy types allowed the system to be further evaluated in greater detail.

In summary, the participants of the study were guided through a practice trial before their results were recorded for this study. The participant produced 40 commands before the trial started, and 40 commands for each of the three trials. Where 20 commands were random, and 20 commands were the same trigger command and all within the 10-minute game limit.

IV. RESULTS AND DISCUSSION

A. Results

Fig.7. shows the results from 14 participants. The group mean accuracy of combination commands was 72.08%, with a maximum accuracy of 95% and a minimum of 57.5%. The average group time to complete the 40 commands was 185.7 seconds(s) with the slowest time at 528 s and the fastest at 71 s.

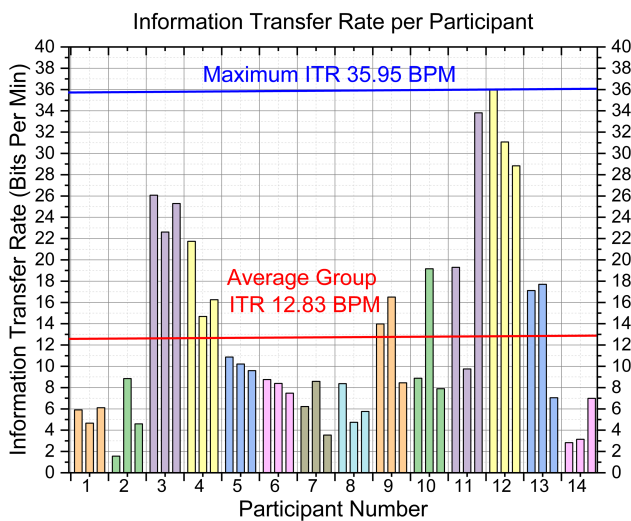


Fig.8. Based on the results from each trial, the Information transfer rate (ITR) was calculated and graphed above. The mean average ITR in bits per min (BPM) of the group was 12.83 BPM. Where participant 12 achieved the maximum ITR of 35.95 BPM.

The time per move was 4.64 s for the group average, with the slowest at 13.2 s and fastest at 1.77 s per move. For the stimuli-only accuracy, the group average was 44.45% with the maximum at 90% and minimum at 15%. The information transfer rate (ITR) or bit rate calculated using formulae found from [40], [41], are of the 4 command options (right, left, both, trigger) across the 40 commands and for the group average was 12.83 bits per minute (BPM). As shown in Fig.8, the peak ITR was calculated to be 35.95 BPM and the minimum 1.56 BPM.

B. Discussion

All participants from their trials were able to complete the game within the 10-minute time limit. Therefore, the minimum combination accuracy was at least 50%. This showed that each participant managed to blink their right eye individually followed by any eyeblink command. Furthermore, since participant 11 had a near perfect score (38/40) also showed that it was possible for an individual to achieve high accuracy. Where 3 participants (3,11 and 12) from 4 out of 9 trials had achieved high stimuli accuracy at 70% or above and had completed the game between 80-116 secs. This is faster than the group average, therefore slower speeds did not indicate better accuracy.

In comparison, 9 different participants (1, 2, 5, 6, 7, 8, 10, 13, 14) from 16 trials achieved 35% or less, meaning if the participant did the same eyeblink of the three available command options for all the game-stimuli, then they would achieve 7 out of 20 or 35% (round up from 33%). However, the stimuli were randomly selected, and the three options were not equally distributed per trial. Hence, it would mean some intentional correct moves that matched the stimuli may have been present from the 9 participants. Likewise, if the participant only did a single command, then they may also be able to achieve more than 35%. It must be noted during testing, no single participant used the same command for all their stimuli, and everyone had the opportunity to try all the three commands for each trial conducted.

One of the main reasons for low accuracy levels from the participants was the inability to continually wink purposefully.

Some had difficulty winking and keeping their head still after triggering, occasionally. Where some had issues winking a certain eye at some instances or fatigue would set in. Those that relayed they had issues making individual blinks or blink a certain eye, were participants, 1, 2, 5, 6, 7, 13 and 14. These group of participants had a stimuli-only average accuracy of 36.19% with peak accuracy at 55%. Therefore, the 7 participant's inclusion, had meant the group mean average would decrease. If the 7 participants with reported issues had each of their 3 trials omitted, the 7 remaining participants without reported winking issues would have a better stimuli-only group average of 52.17%, or a combination accuracy of 76.07%.

Another factor to consider is fatigue, as participants 2, 7 and 8 found the test fatiguing. Participants 2, 7 also shared that they had difficulty individually blinking, whereas participant 8 did not. Each participant took longer than the group average, where participant 2 had the following time and stimuli accuracy results (528 s (15%), 237 s (55%), 301 s (35%)). Participant 2 had shown great improvement between trials 1 and 2, whilst the third trial had a decrease in performance. Participant 7 had the following results (248 s (40%), 200 s (45%), 232 s (15%)). Participant 7 between trial 1 and 2 had shown marginally better accuracy and faster speeds, whilst by trial 3 had reduced their accuracy considerably from trial 2 and with slower speed. Participant 8 had the following results (165 s (35%), 259 s (30%), 268 s (40%)). Participants 2 and 7 had shown a decrease in performance from both slower speeds to complete the trial and the stimuli-only accuracy. It may suggest the addition of a third trial may be straining. Whilst participant 8 data did not support the hypothesis, as from trial 2 and 3 only the elapsed time had worsened, whilst the accuracy was improved by 10%. Participant 8 elapsed time had severely worsened at trial 3 compared from trial 1 by almost 100 seconds, this suggests that fatigue can be a factor in worsening of performance either through slower speeds or accuracy after each consecutive trial.

After each trial, fatigue is not the only factor that may affect performance, where after each trial a person can improve performance through practise. A good figure of merit, that takes accuracy and time into consideration is the ITR [49], [50], as shown in Fig.8. Where from the first and third trial, 4 participants 1 (5.9, 6.11 BPM), 2 (1.56, 4.59 BPM), 11 (19.3, 33.81 BPM) and 14 (2.83, 6.99 BPM) had improved performance, whilst 10 participants did not. When comparing trial 1 and 2 only, 6 participants had improved performance whilst 8 participants did not. The participants were 2 (1.56, 8.85 BPM) 7 (6.22, 8.59 BPM) 9 (13.98, 16.51 BPM) 10 (8.88, 19.16 BPM) 13 (17.11, 17.9 BPM) 14 (2.83, 3.14 BPM). This shows that between trial 1 and 2, 42% of participants had a better understanding of the game, yet the majority did not.

One of the key issues for the low numbers of improved performances was the lack of feedback after each stimulus. The main reason reaching this hypothesis was that all the participants 1-14, found the lack of feedback was the main cause for the difficulty of the game. As only the trigger command would be indicated, whilst the other three LEDs (sensor threshold LEDs), as shown in Fig.6, would light up - only when threshold is met. The LEDs did not indicate if the previous eyeblink command had correctly matched the stimuli, nor was any other mechanism was present for the participant to

TABLE I
PERFORMANCE SUMMARY AND COMPARISON TABLE OF THIS WORK WITH THE STATE-OF-THE-ART.

Reference	Measured Target	Sensor Technology	Sensor package	Light Sensitive	Mobility	Number of User Input Actions	Number of Target Commands	Cost In GBP	Number of Test Users	Mean Accuracy	ITR (bits/min)
Nakanishi <i>et al.</i> 2018	Brain Activity + eye artifacts detection	9 Electro-encephalography (EEG) Electrodes + camera. (SSVEP)	PC based camera+ Electrode cap	No	Very Low	40 frequencies	40	Unknown	20	89.83%	325.33
Mannan <i>et al.</i> 2020	Brain Activity+ eye gaze hybrid	9 EEG Electrodes + camera. (SSVEP)	PC based camera + Electrode cap	No	Very Low	6 frequencies and 8 gaze locations.	48	Unknown	20	90.35%	184.06
Fathi <i>et al.</i> 2015	Video eyeblink	720P Web camera	PC based camera setup	Yes	Very Low	2 (slow & fast blink)	15	Camera (£20) excluding PC	30 (Offline Classification)	97%	Not Available
Sato <i>et al.</i> 2017	Video eyeblink	Camera (1080p, 60FPS)	PC based camera setup	Yes	Very Low	3 (involuntary, slow & fast)	3	£60 excluding PC	10	95%	Not Available
You <i>et al.</i> 2017	Video eyeblink	Infrared video	PC based Infrared camera setup	No	Very Low	3 (very slow, slow & fast)	3	£500 excluding PC	200 (Offline Classification)	91.6%	Not Available
Singh <i>et al.</i> 2018	Video eyeblink	720P Web camera	PC based camera setup	Yes	Very Low	3 (left, right & both eyes)	3	Camera (£20) excluding PC	10	89%	Not Available
Kowalczyk <i>et al.</i> 2018	Video eyeblink	Infrared video	Two Infrared cameras mounted on glasses	No	Medium mobility, requires USB Wire	3 (left, right & both eyes)	3	Estimated £1000 excluding PC	30	99.68%	Not Available
Huang <i>et al.</i> 2018	Eyeblink	Electro-oculography (EOG)	Electrode, processing box on Wheelchair	No	Medium, requires wheelchair	3 (left, right & both eyes)	13	EOG estimated £1250 excluding PC	8	96.7%	57.3
Graybill <i>et al.</i> 2019	Eyeblink	Inductive	Wearable glasses & coil on eyelid	No	High (wearable)	3 (left, right & both eyes)	6	Unknown ("low cost")	6	96.3%	56.1
This Work	Eyeblink	Magnetic sensor	Sensor on wearable glasses & magnet on eyelid	No	High (wearable)	3 (left, right & both eyes)	4	£60 approx. Excluding PC	14	Avg. 72.08% Max. 95%	Avg. 12.83 Max. 35.95

check their progress during each trial. The importance of feedback to improve performance have been highlighted in medical journals such as [42], [43]. Therefore, the stimuli game would benefit having a feedback mechanism during each trial.

Other issues with the stimuli game may have also affected performance, where participant 10 had known threshold issues. Since prior to testing, required that the researcher manually set the threshold for the participant, and it was not changed after each trial. This caused the interface not to register an eyeblink, when the participant clearly had blinked. Human error can affect the results when setting the threshold and as such participant 10 had less than 30% stimuli-only accuracy in trial 1 and 3. Where trial 2 did have a stimuli-only accuracy of 60% meaning at some instance, the participant did meet the threshold occasionally but the overall likelihood during the three trials was only minor.

It must be mentioned that participants 2, 10 and 11, wore sight correction glasses, and had taken them off during the trials. The gesture eyewear was not used with their glasses, participant 2 and 10 opted to take them off since the stimuli indicator were both auditory and the LED indicators were large. Whereas

participant 8, wore eye contact lens during the trial. The average stimuli accuracy from participants that removed their glasses was 46.66% and was higher than the group average 44.4%. This suggests when comparing as a group, those that took their glasses off did not suffer in terms of stimuli-only accuracy.

C. Comparison

Table 1 modified from Tanwear *et al.* [44], compares seven eyeblink studies and two studies that detect brain activity for human computer interaction (HCI) [18], [36], [41], [45]–[50]. The table has two metrics that compares the performance of the different types of HCI devices, accuracy and ITR. Our system has a group mean average of 72.08% and the ITR of 12.83 bits/min, small when comparing to the table. The rest of the table has a minimum accuracy of 89%, the maximum is at 99.68% and are averaged at 93.94%. As explained earlier, the low group-mean-accuracy can be attributed to individuals having issues winking as an example, and since only one individual could achieve accuracy higher than 93.94%. Any future studies will need to improve the accuracy and be up-to-par with examples shown in the table. Investigating different classification methods and optimising the amplitude-threshold

classifier are two examples that any future studies can implement.

The number of participants (14) for this work was almost double than the other non-visual eyeblink technologies. This however may not be the main reason for a low ITR when comparing to the non-visual eyeblink studies. The low ITR could be attributed to the small number of target command options (4) and compared to other eyeblink studies from the table it was the lowest, and thus lowered the ITR. For example, if participant 12 with an ITR of 35.95 bits/min, still had an accuracy of 87.5% from 40 commands and still completed the trial within 84 seconds, they could have achieved an ITR of 50.03 bits/min if the number of command targets options were 6. Or with 13 command targets, an ITR of 77.39 bits/min could have been possible.

The highest ITR from the table was found in studies that use a spelling interface, Nakanishi *et al.* [45], achieved 325.33 bits/min with 40 targets and Mannan *et al.* [41], 184.06 bits/min with 48 targets. There were 9 electrodes and a camera for both studies to allow a greater number of user-inputs, hence it was significantly higher than what the eyeblink technologies could offer. Specifically, for Nakanishi *et al.*, [45], the 9 electrodes were detecting 40 different frequency bandwidths and a camera for detecting eye movement artifacts, whilst for Mannan *et al.* [41], 6 different frequency bandwidths were detected and a camera was used for eye gaze classification, for 8 different locations. The increased number of user-inputs allowed the system to have a higher number of targets and hence ITR, something which the eyeblink systems with two sensors, that only detect eyelid movement had difficulty achieving. It must be noted the time to complete each trial affected the ITR as well, for example using a low number of inputs, that use repeating combination of user-inputs for a single command target, would also reduce the ITR [40], [41].

This study has other advantages from most other systems, such as this system and Graybill *et al.* have high mobility [36]. They are both considered a wearable eyewear device and are insensitive to light conditions, and hence can be used indoors or outdoors. They both have Bluetooth capabilities that can be used with mobile phones or other wireless devices. Another advantage of this work and some other systems such as from Fathi *et al.*, Sato *et al.* and Singh *et al.* were the low costs, approximately £60 or less [18], [46], [48]. Whilst others were considered expensive over £500 or have cost that are not calculated, Nakanishi *et al.*, Mannan *et al.* are ‘Unknown’ but are likely to be costly, whilst Graybill *et al.* likely to be ‘low cost’ [36], [41], [45].

In summary, when comparing to other technologies in this table, this study shows the system has one of the lowest costs, a high mobility and is insensitive to light conditions. If this work improves the accuracy from individuals e.g., with winking difficulties it can then improve the average mean accuracy and ITR, making it a more competitive eyeblink device. This includes exploring other classification methods or optimising the current threshold-based algorithm to account for different individuals’ abilities. Combining improved accuracy and an additional number of target commands that the algorithm can translate, from three inputs (right wink, left wink and both blinks) to at least six target commands, will increase the ITR considerably.

V. LIMITATIONS AND FUTURE WORK

The aim of the eyeblink detection system was to highlight the feasibility of such a system, from the eyewear design down to the circuit components, a more sustainable device can emerge from future iterations. Things that were limited in this study or are needed in the future iteration are briefly highlighted below:

A. Calibration and Classification: As stated in the previous sections. The threshold was manually set, and that human error can affect the probability that a blink will not be registered or that the neighbouring sensor would pick up the change in magnetic field. It is recommended that an auto-calibration algorithm should be developed to counteract human error. Where manually setting the threshold can be challenging, as changing the position of the magnetic strip meant that the system would need to be recalibrated, each time a magnetic strip was reused. Also, mentioned in the discussion, the lack of a feedback mechanism had meant that the participant found the game difficult, having a progress indicator should improve the results for the threshold classifier. If it was found that amplitude threshold-based classification is still lacking, then other types of classification methods should also be explored, for example a pattern may emerge from different individuals, where the incorrect eye would blink first, followed by the correct eye. And as such a machine learning algorithm based on larger datasets can be adopted to improve performances in terms of accuracy.

B. Multiple command functionality: Implementing machine learning classification or optimising the current threshold-based classifier should increase accuracy, to allow a chain of user-inputs to translate into more command targets. The system in this paper had four command targets, trigger, right, left, and both eyeblinks from two inputs (right and left eye). More command targets are needed to interface with complex applications highlighted in Fig.1. e.g., gaming, wheelchair, car controller. In literature, it was found that the systems based on blinking, the number of command targets can be increased up to 8 by having three repeated commands within a time window, as found in [36]. Having more command targets increases the ITR significantly. The main benefit of having more command targets is that a more complex interface systems can be developed. Whilst the trade-off is that by using longer user-input chains for a single command target, will increase the time to complete a set trial and will then reduce the ITR, therefore further studies are required for comparisons.

C. Cost and Power consumption: The design philosophy of the circuit-designs was a millimetre-range footprint to allow hand soldering, and the choice of components were low noise devices to maximize the signal-to-noise ratio. Other than the sensor and 3D printed eyewear, which were fabricated in-house and were hard to calculate the true costs for, the other components were bought off-the-shelf and were less than £120 GBP. £60 GBP was the estimated cost per eyewear, as the £120 GBP was to cover the cost of spare components, in case of failures.

The chosen components were also compared to achieve low power requirements so that a single lightweight 3.7 V battery source can be used (800mAh, 19 grams). The current consumption of the system, apart from the sensors that at 3.3 V consumed 10 mA each and the microcontroller at 11 mA (5 V),

the high current consumption (0.125A) mainly came from using the voltage divider splitting the 12 volts to +6 V/-6 V. This can be remedied by using a split-supply converter that can output bipolar voltage from a single supply source, this will remove the need for voltage dividers and decrease the current consumption considerably. Where currently 6.6 hours of battery life was provided, it is estimated that least 24 hours of battery life is possible, if the voltage divider using resistors were replaced by a split-supply DC-DC converter, this is based on an estimated consumption of 32 mA using a 3.7 V battery. However, signal analysis is still required as these are typically based on switching regulators and may induce high frequency noise within the system.

D. Wearability of the system: To apply the magnetic strip to the eyelid requires an individual to look into a mirror and attach the strip at the correct position. This would mean that for an impaired or elderly individual, they will need to ask for assistance, as the magnetic strip is small and can be difficult for the individuals to self-apply. Whilst the eyewear will be easier, individuals with the loss of upper limb functions will still need assistance in both cases.

E. Human Physiology and Demographic Inclusions:

This study had limitations on exploring some of the details on the precise nature of human physiology and its physical anatomy difference with respect to eyeblinks. Furthermore, during the testing of the device, children, disabled patients, and the elderly were not present in this study. In principle, the proposed system could be similarly effective for them, if their eyelids are healthy. This study does not compare and analyse blink rate variability, as discussed earlier e.g., individuals with glaucoma had slower blink rates compared to healthy ones.

Given the small size of the cohort (14 participants), the effects of different demographics on the system needs to be explored further. This is because either zero or a small sample of the different types of gender, age and ethnicity were present. Therefore, statistically no claim can be made that one-demographic group had shown to be at an advantage over the other in this study. For example, eyelid shapes and sizes as discussed earlier vary with ethnicity and age. In this study participants from different ethnic groups were present, however it was not explored in this study. Participants that had Caucasian-European ethnicity were (participant 7,8,9,10,12), East-Asian (participant 2,3,4,5,11), South-east Asian (participant 13), south-Asian (participant 1 ,14) and middle eastern (participant 6). However, they were not differentiated and analysed in this study.

In summary, future studies will need to expand this work and compare it with the latest literature that use different measuring instruments to measure blink rates for different demographics. The studies will need to include magnetic size limitations for the different demographics and discover if there is a one-size-fit-all for magnetic strips that can still be detected by the spintronic TMR sensors. Human physiology and technology interaction would also need to be closely analysed, the study needs to understand the principles behind involuntary eyeblinks and possibly removing the need for trigger commands, i.e., to discover if involuntary blinking can be removed by analogue or digital methods such as machine pattern learning algorithms.

VI. CONCLUSION

In this study, 14 volunteers participated in testing our eyeblink gesture system, which was based on magnetic sensing of eyelid magnetic strips. These N42 neodymium magnets were 3 mm in diameter, 0.5 mm thick and were attached to each eyelid using medical tape to fit an adult-age demographic. These magnets were detected using lab-fabricated tunnelling magnetoresistance (TMR) bridge sensors with sensitivity of 14 mV/V/Oe. Due to the repeatability of each eyeblink, amplitude threshold classifier was used. However, it is recommended to use automatically calibrated threshold and machine learning pattern recognition, for improved accuracy for the different types of blinking patterns and to reduce human error when setting thresholds. In this study, the peak combined accuracy from a participant was 95% with the group mean accuracy of 72%, out of a possible 40 commands. The mean elapsed time for all 14 participants to complete each of the three trials was 185 seconds. Moreover, the maximum information transfer rate (ITR) of each participant was 35.95 bits per minute with the group average at 12.83 BPM. The use of highly sensitive spintronic TMR sensors in this study highlight the sensor's versatility within the field of medical science. The impact of such a technology in this study show that with further optimisation of the system, the sensor and its wearable system can be used for clinical trials studying eyeblinks or improving the quality-of-life for individuals, such as those undergoing body injury rehabilitation.

APPENDIX

The LabVIEW program (2019 + newer versions), eyewear design (STL and 3mf files) and Arduino 1.8.13 code (.ino) for the eyelid gesture system are found in the following repository: <https://github.com/melabglasgow/Spintronic-Eyeblink-Gesture-Sensor-with-Wearable-Interface-System> .

The BLE toolkit to interface BLE Devices with LabVIEW is made available from: <https://github.com/MuSAELab/BLE-Toolkit-LabVIEW> .

REFERENCES

- [1] E. L. Graczyk, L. Resnik, M. A. Schiefer, M. S. Schmitt, and D. J. Tyler, 'Home Use of a Neural-connected Sensory Prosthesis Provides the Functional and Psychosocial Experience of Having a Hand Again', *Scientific Reports*, vol. 8, no. 1, p. 9866, Jun. 2018, doi: 10.1038/s41598-018-26952-x.
- [2] F. M. Petrini *et al.*, 'Sensory feedback restoration in leg amputees improves walking speed, metabolic cost and phantom pain', *Nature Medicine*, vol. 25, no. 9, pp. 1356–1363, Sep. 2019, doi: 10.1038/s41591-019-0567-3.
- [3] K. Z. Zhuang *et al.*, 'Shared human–robot proportional control of a dexterous myoelectric prosthesis', *Nature Machine Intelligence*, vol. 1, no. 9, pp. 400–411, Sep. 2019, doi: 10.1038/s42256-019-0093-5.
- [4] B. E. Lawson, J. Mitchell, D. Truex, A. Shultz, E. Ledoux, and M. Goldfarb, 'A Robotic Leg Prosthesis: Design, Control, and Implementation', *IEEE Robotics Automation Magazine*, vol. 21, no. 4, pp. 70–81, Dec. 2014, doi: 10.1109/MRA.2014.2360303.
- [5] S. Dowiasch, S. Marx, W. Einhäuser, and F. Bremmer, 'Effects of aging on eye movements in the real world', *Front. Hum. Neurosci.*, vol. 9, p. 46, 2015, doi: 10.3389/fnhum.2015.00046.

- [6] D. Wendt, T. Brand, and B. Kollmeier, 'An Eye-Tracking Paradigm for Analyzing the Processing Time of Sentences with Different Linguistic Complexities', *PLoS ONE*, vol. 9, no. 6, p. e100186, Jun. 2014, doi: 10.1371/journal.pone.0100186.
- [7] S. He and Y. Li, 'A Single-Channel EOG-Based Speller', *IEEE Transactions on Neural Systems and Rehabilitation Engineering*, vol. 25, no. 11, pp. 1978–1987, Nov. 2017, doi: 10.1109/TNSRE.2017.2716109.
- [8] S. Gulyás, 'Electro-Oculography (EOG) Examination of Eye Movements', in *Neuro-Ophthalmology*, J. Somlai and T. Kovács, Eds. Cham: Springer International Publishing, 2016, pp. 287–293. doi: 10.1007/978-3-319-28956-4_33.
- [9] Y. Cheung and Q. Peng, 'Eye Gaze Tracking With a Web Camera in a Desktop Environment', *IEEE Trans. Human-Mach. Syst.*, vol. 45, no. 4, pp. 419–430, Aug. 2015, doi: 10.1109/THMS.2015.2400442.
- [10] R. Kredel, C. Vater, A. Klostermann, and E.-J. Hossner, 'Eye-Tracking Technology and the Dynamics of Natural Gaze Behavior in Sports: A Systematic Review of 40 Years of Research', *Front. Psychol.*, vol. 8, p. 1845, Oct. 2017, doi: 10.3389/fpsyg.2017.01845.
- [11] M. Dursun *et al.*, 'A new approach to eliminating EOG artifacts from the sleep EEG signals for the automatic sleep stage classification', *Neural Comput. & Applic.*, vol. 28, no. 10, pp. 3095–3112, Oct. 2017, doi: 10.1007/s00521-016-2578-z.
- [12] H. Manabe, M. Fukumoto, and T. Yagi, 'Direct Gaze Estimation Based on Nonlinearity of EOG', *IEEE Transactions on Biomedical Engineering*, vol. 62, no. 6, pp. 1553–1562, Jun. 2015, doi: 10.1109/TBME.2015.2394409.
- [13] B. V. Ehinger, K. Groß, I. Ibs, and P. König, 'A new comprehensive eye-tracking test battery concurrently evaluating the Pupil Labs glasses and the EyeLink 1000', *PeerJ*, vol. 7, p. e7086, Jul. 2019, doi: 10.7717/peerj.7086.
- [14] D. Ivanchenko, K. Rifai, Z. M. Hafed, and F. Schaeffel, 'A low-cost, high-performance video-based binocular eye tracker for psychophysical research', *JEMR*, vol. 14, no. 3, May 2021, doi: 10.16910/jemr.14.3.3.
- [15] 'Tobii Pro Glasses 2 wearable eye tracker', Jun. 25, 2015. <https://www.tobii.com/product-listing/tobii-pro-glasses-2/> (accessed Jun. 08, 2020).
- [16] H. Yamamoto, A. Sato, and S. Itakura, 'Eye tracking in an everyday environment reveals the interpersonal distance that affords infant-parent gaze communication', *Sci. Reports*, vol. 9, no. 1, p. 10352, Jul. 2019, doi: 10.1038/s41598-019-46650-6.
- [17] V. K. Jaswal, A. Wayne, and H. Golino, 'Eye-tracking reveals agency in assisted autistic communication', *Scientific Reports*, vol. 10, no. 1, p. 7882, May 2020, doi: 10.1038/s41598-020-64553-9.
- [18] A. Fathi and F. Abdali-Mohammadi, 'Camera-based eye blinks pattern detection for intelligent mouse', *SIViP*, vol. 9, no. 8, pp. 1907–1916, Nov. 2015, doi: 10.1007/s11760-014-0680-1.
- [19] S. L. Rogers, C. P. Speelman, O. Guidetti, and M. Longmuir, 'Using dual eye tracking to uncover personal gaze patterns during social interaction', *Scientific Reports*, vol. 8, no. 1, p. 4271, Mar. 2018, doi: 10.1038/s41598-018-22726-7.
- [20] A. Tanwear, H. Heidari, E. Paz, T. Bohnert, and R. Ferreira, 'Eyelid gesture control using wearable tunnelling magnetoresistance sensors', *ICECS 2020 - 27th IEEE International Conference on Electronics, Circuits and Systems, Proceedings*, vol. 9781728160, no. October, pp. 23–25, 2020, doi: 10.1109/ICECS49266.2020.9294878.
- [21] M. J. Cartwright, U. R. Kurumety, C. C. Nelson, B. R. Frueh, and D. C. Musch, 'Measurements of upper eyelid and eyebrow dimensions in healthy white individuals', *Am. J. Ophthalmol.*, vol. 117, no. 2, pp. 231–234, Feb. 1994, doi: 10.1016/s0002-9394(14)73081-8.
- [22] K. M. Price, P. K. Gupta, J. A. Woodward, S. S. Stinnett, and A. P. Murchison, 'Eyebrow and Eyelid Dimensions: An Anthropometric Analysis of African Americans and Caucasians', *Plastic and Reconstructive Surgery*, vol. 124, no. 2, pp. 615–623, Aug. 2009, doi: 10.1097/PRS.0b013e3181adde98.
- [23] D. H. Park, W. S. Choi, S. H. Yoon, and C. H. Song, 'Anthropometry of Asian Eyelids by Age', *Plastic and Reconstructive Surgery*, vol. 121, no. 4, pp. 1405–1413, Apr. 2008, doi: 10.1097/01.prs.0000304608.33432.67.
- [24] C. Constable, 'Earth's Electromagnetic Environment', *Surveys in Geophysics*, vol. 37, no. 1, pp. 27–45, Jan. 2016, doi: 10.1007/s10712-015-9351-1.
- [25] D.-K. Li, H. Chen, J. R. Ferber, R. Odouli, and C. Quesenberry, 'Exposure to Magnetic Field Non-Ionizing Radiation and the Risk of Miscarriage: A Prospective Cohort Study', *Sci Rep*, vol. 7, no. 1, p. 17541, Dec. 2017, doi: 10.1038/s41598-017-16623-8.
- [26] I. C. on N.-I. R. Protection, 'GUIDELINES ON LIMITS OF EXPOSURE TO STATIC MAGNETIC FIELDS', *Health Physics*, vol. 96, no. 4, pp. 504–514, Apr. 2009, doi: 10.1097/01.HP.0000343164.27920.4a.
- [27] 'Radiation: Electromagnetic fields'. <https://www.who.int/news-room/questions-and-answers/item/radiation-electromagnetic-fields> (accessed Mar. 12, 2022).
- [28] E. Paz, R. Ferreira, and P. P. Freitas, 'Linearization of Magnetic Sensors With a Weakly Pinned Free-Layer MTJ Stack Using a Three-Step Annealing Process', *IEEE Transactions on Magnetics*, vol. 52, no. 7, pp. 1–4, Jul. 2016, doi: 10.1109/TMAG.2016.2525772.
- [29] S. Cardoso *et al.*, 'Magnetic tunnel junction sensors with pTesla sensitivity for biomedical imaging', in *Smart Sensors, Actuators, and MEMS VI*, May 2013, vol. 8763, p. 87631A. doi: 10.1117/12.2018070.
- [30] E. Paz, S. Serrano-Guisan, R. Ferreira, and P. P. Freitas, 'Room temperature direct detection of low frequency magnetic fields in the 100 pT/Hz0.5 range using large arrays of magnetic tunnel junctions', *Journal of Applied Physics*, vol. 115, no. 17, p. 17E501, Jan. 2014, doi: 10.1063/1.4859036.
- [31] R. Guerrero, M. Pannetier-Lecoeur, C. Fermon, S. Cardoso, R. Ferreira, and P. P. Freitas, 'Low frequency noise in arrays of magnetic tunnel junctions connected in series and parallel', *Journal of Applied Physics*, vol. 105, no. 11, 2009, doi: 10.1063/1.3139284.
- [32] P. P. Sharma, E. Albisetti, M. Monticelli, R. Bertacco, and D. Petti, 'Exchange Bias Tuning for Magnetoresistive Sensors by Inclusion of Non-Magnetic Impurities', *Sensors (Basel)*, vol. 16, no. 7, Jul. 2016, doi: 10.3390/s16071030.
- [33] J. Cao and P. P. Freitas, 'Wheatstone bridge sensor composed of linear MgO magnetic tunnel junctions', *Journal of Applied Physics*, vol. 107, no. 9, p. 09E712, May 2010, doi: 10.1063/1.3360583.
- [34] F. Franco, S. Cardoso, and P. P. Freitas, 'Reconfigurable Spintronics Wheatstone Bridge Sensors With Offset Voltage Compensation at Wafer Level', *IEEE Transactions on Magnetics*, vol. 55, no. 7, pp. 1–5, Jul. 2019, doi: 10.1109/TMAG.2019.2896379.
- [35] Z. Jin, M. A. I. Mohd Noor Sam, M. Oogane, and Y. Ando, 'Serial MTJ-Based TMR Sensors in Bridge Configuration for Detection of Fractured Steel Bar in Magnetic Flux Leakage Testing', *Sensors (Basel)*, vol. 21, no. 2, p. 668, Jan. 2021, doi: 10.3390/s21020668.
- [36] P. Graybill and M. Kiani, 'Eyelid Drive System: An Assistive Technology Employing Inductive Sensing of Eyelid Movement', *IEEE Trans. Biomed. Circuits Syst.*, pp. 1–1, 2018, doi: 10.1109/TBCAS.2018.2882510.
- [37] R. Paprocki and A. Lenskiy, 'What Does Eye-Blink Rate Variability Dynamics Tell Us About Cognitive Performance?', *Front. Hum. Neurosci.*, vol. 11, 2017, doi: 10.3389/fnhum.2017.00620.
- [38] Y. Wang, S. S. Toor, R. Gautam, and D. B. Henson, 'Blink Frequency and Duration during Perimetry and Their Relationship to Test-Retest Threshold Variability', *Invest. Ophthalmol. Vis. Sci.*, vol. 52, no. 7, pp. 4546–4550, Jun. 2011, doi: 10.1167/iovs.10-6553.

- [39] K.-A. Kwon *et al.*, ‘High-speed camera characterization of voluntary eye blinking kinematics’, *J R Soc Interface*, vol. 10, no. 85, p. 20130227, Aug. 2013, doi: 10.1098/rsif.2013.0227.
- [40] B. Dal Seno, M. Matteucci, and L. T. Mainardi, ‘The Utility Metric: A Novel Method to Assess the Overall Performance of Discrete Brain–Computer Interfaces’, *IEEE Transactions on Neural Systems and Rehabilitation Engineering*, vol. 18, no. 1, pp. 20–28, Feb. 2010, doi: 10.1109/TNSRE.2009.2032642.
- [41] M. M. N. Mannan, M. A. Kamran, S. Kang, H. S. Choi, and M. Y. Jeong, ‘A Hybrid Speller Design Using Eye Tracking and SSVEP Brain–Computer Interface’, *Sensors (Basel)*, vol. 20, no. 3, p. 891, Feb. 2020, doi: 10.3390/s20030891.
- [42] D. Z. Hambrick, B. N. Macnamara, and F. L. Oswald, ‘Is the Deliberate Practice View Defensible? A Review of Evidence and Discussion of Issues’, *Front Psychol*, vol. 11, p. 1134, Aug. 2020, doi: 10.3389/fpsyg.2020.01134.
- [43] G. Tzetzis, E. Votsis, and T. Kourtessis, ‘The Effect Of Different Corrective Feedback Methods on the Outcome and Self Confidence of Young Athletes’, *J Sports Sci Med*, vol. 7, no. 3, pp. 371–378, Sep. 2008.
- [44] A. Tanwear *et al.*, ‘Spintronic Sensors Based on Magnetic Tunnel Junctions for Wireless Eye Movement Gesture Control’, *IEEE Transactions on Biomedical Circuits and Systems*, 2020, doi: 10.1109/TBCAS.2020.3027242.
- [45] M. Nakanishi, Y. Wang, X. Chen, Y.-T. Wang, X. Gao, and T.-P. Jung, ‘Enhancing Detection of SSVEPs for a High-Speed Brain Speller Using Task-Related Component Analysis’, *IEEE Trans Biomed Eng*, vol. 65, no. 1, pp. 104–112, Jan. 2018, doi: 10.1109/TBME.2017.2694818.
- [46] H. Sato, K. Abe, S. Ohi, and M. Ohyama, ‘An Automatic Classification Method for Involuntary and Two Types of Voluntary Blinks’, *Electronics and Communications in Japan*, vol. 100, no. 10, pp. 48–58, 2017, doi: 10.1002/ecj.11986.
- [47] F. You, Y. Li, L. Huang, K. Chen, R. Zhang, and J. Xu, ‘Monitoring drivers’ sleepy status at night based on machine vision’, *Multimed Tools Appl*, vol. 76, no. 13, pp. 14869–14886, Jul. 2017, doi: 10.1007/s11042-016-4103-x.
- [48] H. Singh and J. Singh, ‘Real-time eye blink and wink detection for object selection in HCI systems’, *J Multimodal User Interfaces*, vol. 12, no. 1, pp. 55–65, Mar. 2018, doi: 10.1007/s12193-018-0261-7.
- [49] P. Kowalczyk and D. Sawicki, ‘Blink and wink detection as a control tool in multimodal interaction’, *Multimed Tools Appl*, vol. 78, no. 10, pp. 13749–13765, May 2019, doi: 10.1007/s11042-018-6554-8.
- [50] Q. Huang *et al.*, ‘An EOG-Based Human–Machine Interface for Wheelchair Control’, *IEEE Transactions on Biomedical Engineering*, vol. 65, no. 9, pp. 2023–2032, Sep. 2018, doi: 10.1109/TBME.2017.2732479.